

Article

Development of a Tree-Shaped Hybrid Nanogenerator Using Flexible Sheets of Photovoltaic and Piezoelectric Films

Rahate Ahmed, Yeongmin Kim, Zeeshan and Wongee Chun * 

Department of Nuclear and Energy Engineering, Jeju National University, Jeju 63243, Korea; rahat@jejunu.ac.kr (R.A.); km820426@jejunu.ac.kr (Y.K.); zeeshan@jejunu.ac.kr (Z.)

* Correspondence: wgchun@jejunu.ac.kr; Tel.: +82-064-754-3646

Received: 29 October 2018; Accepted: 4 January 2019; Published: 12 January 2019



Abstract: This paper reports on the feasibility of a tree-shaped hybrid nanogenerator (TSHG) made of flexible sheets of photovoltaic (PV) and piezoelectric (piezo) films for harnessing both wind and solar energy. The proposed system has been designed to produce electricity if there is any light, wind or strong rainfall. It shows how the power developed by each piezo film sheet was integrated in conjunction with its limited power output which is produced by the sporadic movement of the sheets. Regardless of its magnitude, the AC power output of each piezo film sheet was converted with a full wave bridge rectifier and then passed to a capacitor. The TSHG has an excellent performance with an open circuit voltage of 5.071 V, a short-circuit current of 1.282 mA, and a maximum power output of 3.42 mW at a loading resistance of 5 k Ω . Moreover, a wind driven TSHG was capable of charging a 1000 μ F capacitor, which was subsequently discharged through LED lighting.

Keywords: hybrid nanogenerator; sheets of piezoelectric and photovoltaic films; full wave bridge rectifier; wind energy; solar energy

1. Introduction

Nowadays, the importance of renewable energy production has increased significantly with the increase in global warming [1–3]. The Sun is the most abundant renewable energy source in the world. Solar energy can be exploited in different ways; for example, photovoltaic (PV) power generation is one of the most reliable and widely applied technologies around the world. Solar cells, the basic elements of PVs, are designed to convert photons to electrical energy using the photovoltaic effect [4–6]. The first modern photovoltaic solar cell based on silicon was invented by Russel [7]. First generation solar cells were thin silicon wafers that directly convert light energy into electrical energy. Until the development of a thin film solar cell, silicon wafer-based technology was the most popular. Recent advancement in nanotechnology, however, has given birth to the second generation of solar cells [8,9] with improved performance and flexibility [10,11]. Especially, flexible PV films have significantly expanded the area of solar energy application because they are bendable, easy to handle and adaptable to various operations [12,13]. They enable flexibility in harvesting solar energy for power generation integrated with other means of energy conversion for maximum energy efficiency.

The piezoelectric effect has attracted much attention these days in harnessing small mechanical energy, especially from the wind. Many studies have been done that used PV technology in conjunction with piezoelectric (piezo) materials for the generation of electric power from both solar and wind energy [14–16]. Recently, a single hybrid cell was developed to harvest both solar and mechanical power at the same time [17–19]. A micro-cable structured solar and mechanical energy harvester was proposed by Chen and et al. [20]; they demonstrated its performance by charging a 2 μ F capacitor up to 2V in 1 minute.

During the last decade, technological breakthroughs in the synthesis of piezoelectric materials have expedited the development new designs of piezoelectric nanogenerators [21,22]. Wang and Song successfully introduced an innovative piezoelectric nanogenerator in 2006, which was able to produce several millivolts by bending a ZnO nanowire with the tip of an atomic force microscope (AFM) [23]. This attracted many researchers because it opened a new field in nanoscale applications of piezoelectric materials. Since then, researchers around the world have come up with different designs of nanogenerators for diverse applications focusing on practicability [24–27]. However, in diversifying the electricity generation system, many researchers came up with the idea of simultaneously harnessing wind and solar energy. Kekkogg et al. [28] proposed the optimal unit sizing for a hybrid wind/photovoltaic generating system, in which they investigated a stand-alone and network connected system. In addition, to scavenge wind power by using nanomaterials, Oh et al. [29] proposed a tree shaped generating system. They compared output power by utilizing lead-zirconium-titanium (PZT) and polyvinylidene fluoride (PVDF) films. An r-shaped hybrid nanogenerator was designed and fabricated by Han et al. [30] to enhance piezoelectricity in the presence of triboelectric charges. In their experiment, a power density of 2.04 mW/cm^3 was produced by the triboelectric device while 10.95 mW/cm^3 was produced by the piezoelectric device. For ambient energy scavenging, a flat panel-shaped hybrid piezo/triboelectric nanogenerator was proposed by Hassan et al. [31]. Their hybrid device produced a combined peak voltage of 300 V in an open circuit and a maximum short-circuit current density of 16 mA/cm^3 at 50Ω load.

The present work introduces a high-performance energy harvesting system, which is a tree-shaped hybrid nanogenerator (TSHG) made of flexible solar cells (films) and piezoelectric film sheets. To experimentally fabricate a TSHG, fluorinated ethylene propylene (FEP) films were used to make the structure of leaves. A solar cell was attached to the top surface of each leaf while a sheet of piezo film was attached to its other (bottom) side. To demonstrate its operational characteristics and functional robustness of the TSHG, a capacitor was used to store electricity and then applied to an external load.

2. Operation of the TSHG for Motion and Solar Energy Harvesting

2.1. Fabrication of the Polyvinylidene Fluoride (PVDF) Polymer-Based Leaf

Some single crystal materials show the following phenomenon which describes the operating principle of piezoelectric materials to produce electric potential. Due to the deformation of a crystal by application of an external force, electric charges appear on certain faces of the crystal. When the exerted force is released, the polarity of the electric charge changes [32]. This property of the crystal is called the piezoelectric effect, a typical structure of piezoelectric crystals as shown in Figure 1a. Currently, different types of PVDF based piezoelectric films are available. In the present study, a nanogenerator made of a LDT4-028K/L piezo film was used in conjunction with the reclamation of wind energy. When a sheet of LDT4-028K/L film is induced to bend, it generates voltage proportionate to the degree of bending. Table 1 and Figure 1b give a detailed description of PVDF used in this work. To facilitate the harvesting of wind energy, an artificial tree was made with many leaves, where each leaf had sheets of piezo films attached, as shown in Figure 2b.

Table 1. Dimensions of a piezo film (LDT4-028K/L) [26]

Film Thickness (μm)	A Film (mm)	B Electrode (mm)	C Film (mm)	D Electrode (mm)	Total Thickness (μm)	Capacitor (nF)
28	21	18	170	155.7	205	11

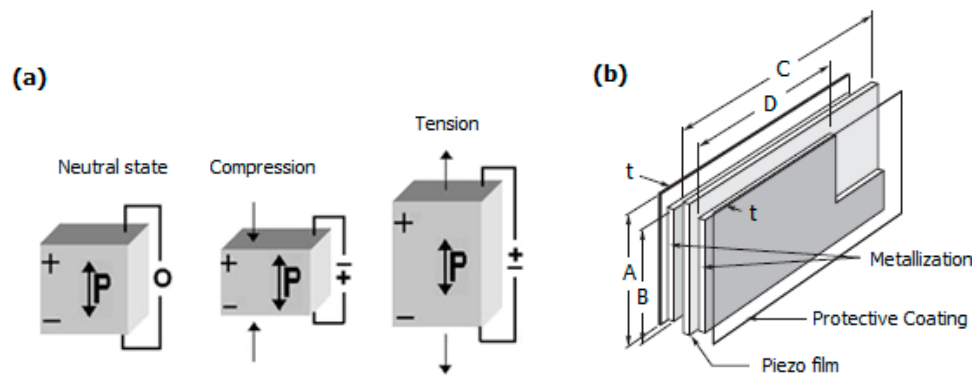


Figure 1. Piezoelectricity: (a) piezoelectric effect generated by an external force [32] (b) dimensions of a piezo film (with reference to Table 1) [26].

2.2. Fabrication of the Photovoltaic Cell Based Leaf

A solar cell converts light energy into electricity by the photovoltaic effect. Hundreds of solar cells make up a photovoltaic array. Solar cells contain materials with semiconducting properties in which their electrons become excited and turn into an electrical current when struck by light energy. Among the many kinds of solar cells, the present study used a thin film solar cell (infinityPV, Ltd., Jyllinge, Denmark) which was fixed onto the surface of a leaf. Figure 2a describes the fabrication process involved in conjunction with exploiting solar energy. Our TSHG has three pieces (110 mm × 50 mm) of leaves with a PV film.

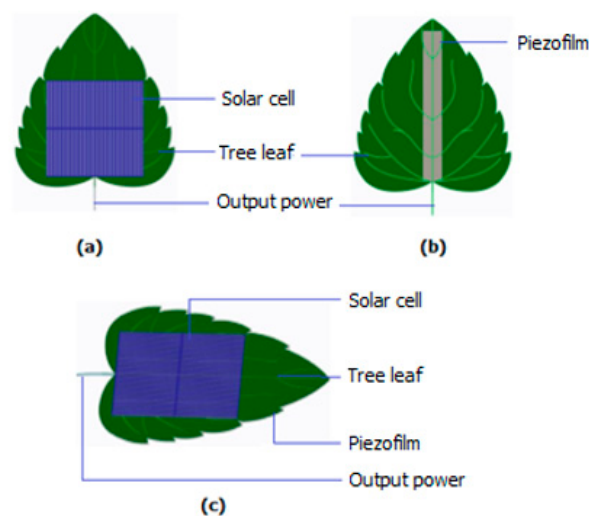


Figure 2. Structure of the generator (a) flexible photovoltaic film affixed onto the surface of a leaf (b) a PVDF film attached with bottom of the leaf (c) photovoltaic film and PVDF film-based leaf.

3. Manufacturing of the TSHG

The main objective of this work was to design a hybrid system that simultaneously converts wind and solar (light) energy into electricity. To implement this, an artificial tree was designed shown in Figure 3. There were ten leaves on the TSHG. Of these, three had both PV and piezo films fixed onto either side of a leaf while each of the remaining leaves was affixed with a sheet of piezo film shown in Figure 2b. By doing this, the TSHG was capable of capturing small disturbances caused by the wind and producing a high voltage for generating electricity. The fine wires to transmit the electricity generated by the sheets of piezo and PV films were placed in the hollow space available at the center of the trunk (hollow pipe). An actuator circuit was installed at the bottom of the tree, where each output

of the generators was integrated. The alternating output power (i.e., AC current) from each sheet of piezo film was transmitted to a bridged rectifier before it was stored in a capacitor.

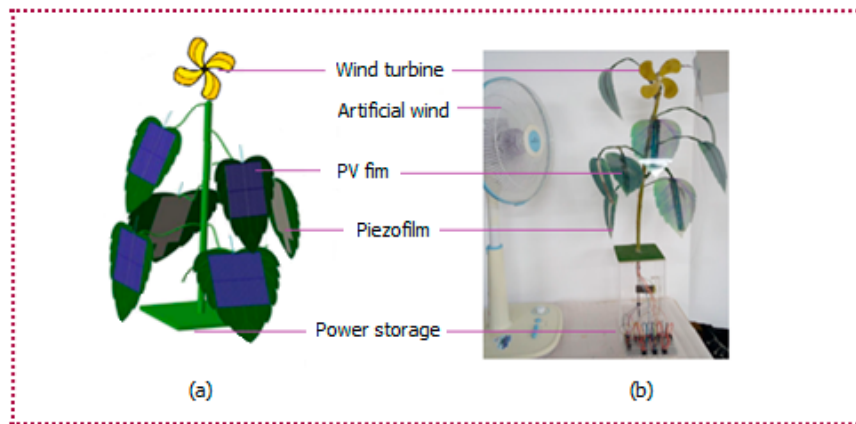


Figure 3. Tree shaped hybrid nanogenerator (TSHG) (a) conceptual design (b) actually fabrication.

Meanwhile, the DC output (DC current) by the PV films was directly used to charge the same capacitor by passing any rectifier. When sheets of both the PV and piezo films were affixed onto a leaf, the leaf was a bit stiffer than the leaves with only sheets of piezo films. It, however, was still bendable by a moderate wind. A series of tests were performed to assess the practicability of the TSHG under various wind speeds using an electric fan shown in Figure 3.

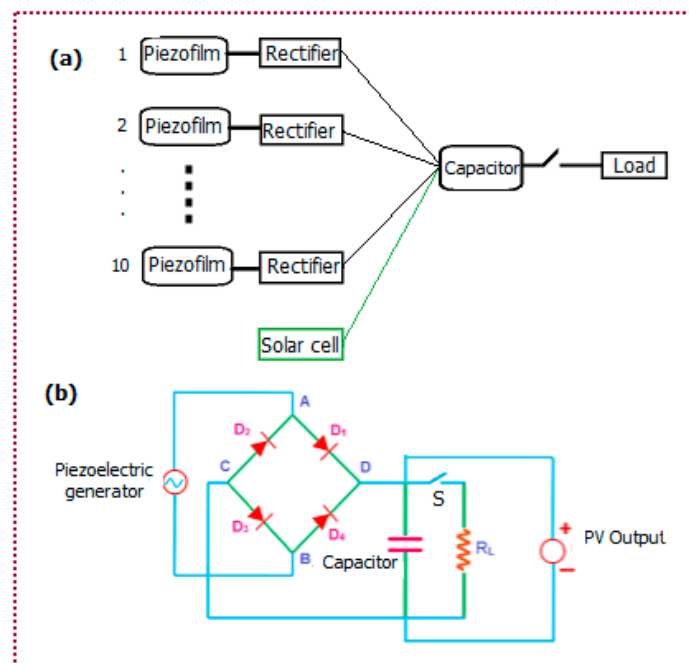


Figure 4. Circuit for the integration of the power output of the TSHG (a) logic diagram (b) power management circuit.

4. Circuit Construction for the TSHG

The power output by the sheets of the PV films was enough to readily run a small electronic device while that by the sheets of the piezo films was insufficient to directly drive a device. This is somewhat expected because each sheet of piezo film is only capable of producing a small power output due to its inherent technical limit. To resolve this, a capacitor was placed before any power

was applied to the load. Figure 4a,b show the logic and actual design details of the constructed circuit for the integration of the PV and piezo power output. For a moderate level of wind speed (7–8 m/s), a single piezo film generates a very small amount of electricity with a very high spike of voltage. To deal with this situation, a full wave bridge rectifier was used to handle the electrical output from a single piezo film; the electrical output was rectified to charge a capacitor. That is, the electrical output of each piezo film was processed with a rectifier before it was integrated with the others to charge a capacitor. Before proposing this power accumulating circuit, attempts were made to integrate the generated AC output power by piezo films without using a separate rectifier circuit. However, this was not feasible for due to sporadic movements of the piezo films and produced very low output power. To overcome this technical problem, the proposed circuit was designed for maximum power accumulation by exploiting the piezo films.

5. Performance Measurement

5.1. Basic Electrical Output of the Piezoelectric Nanogenerator

Before conducting full scale measurements, the basic electrical output from a single piezo film was measured. Even under small wind speeds, a sheet of piezo film was capable of generating electrical signals. A positive potential generates in the circuit when a force applied to a piezo film. Conversely, releasing the applied force created a negative potential in the circuit. Figure 5 shows the output characteristics of a piezoelectric nanogenerator. Figure 5a schematically shows the operation of the nanogenerator, where a force is applied onto and released from a simple piezo film. Subject to the external force applied on the crystal structure, an electrical signal is generated in the connected circuit. The power output of a piezoelectric nanogenerator depends on the magnitude of oscillations induced on the film surface. A short-circuit current generated during the process of applying and releasing a force on a single piezo film is shown in Figure 5b. At wind speeds of 7–8 m/s, a single piezo film generated a short-circuit current of 2.72 μA and an open circuit voltage of 1.2 V. A sample of the rectified electrical output during such a process is shown in Figure 5d.

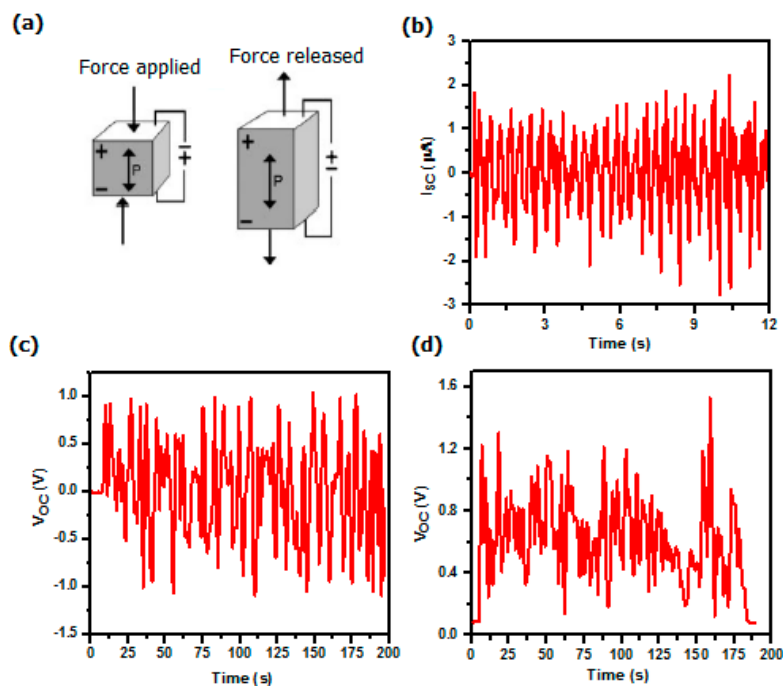


Figure 5. Performance of a simple piezoelectric nanogenerator by a compressive force: (a) a force applied and released on a simple piezo film (b) short-circuit current generated by a single piezo film (c) open circuit voltage generated during the bending and releasing modes (d) rectified open circuit voltage.

Measurements were made for an open circuit with 10 sheets of piezo films connected separately with the rectifier. To simulate mechanical forces on the piezo film in real situations, an electric fan was used generating a steady flow of wind. Different wind speeds were tested to investigate the movement of the leaves as they deform constantly and develop electric power by air flow. At the start of the air flow, large spikes of AC voltage were developed in the piezo films, which were subsequently rectified and integrated to produce an open circuit voltage of 4.89 V and a short-circuit current of 9.32 μA at wind speeds of 7–8 m/s as shown in Figure 6a,b. Further tests were conducted at different operating conditions (wind speeds). At wind speeds ranging from 5 m/s to 6 m/s, the respective integrated open circuit voltage and short-circuit current were recorded to be 2.65 V and 5.94 μA , as shown in Figure 6c,d. For the case of wind speeds between 3 m/s and 4 m/s, the recorded values were 1.68 V and 4.83 μA , respectively, as shown in Figure 6e,f. The output parameters of the piezo films were affected by deviations in wind speed. To investigate the performance characteristics of each piezo film in conjunction with wind directions, a series of tests were conducted repeatedly to find the conditions that give the highest output. These conditions were then adopted to get the maximum power output from the TSHG.

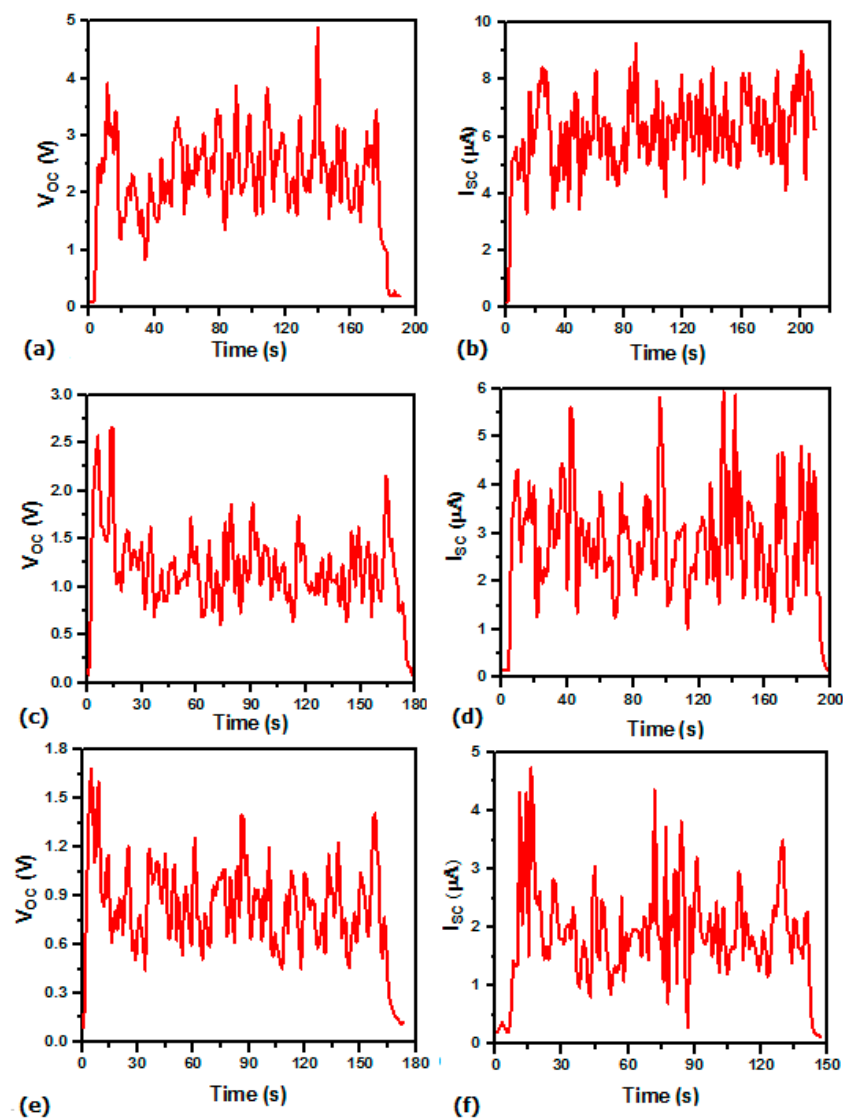


Figure 6. Electrical output of the piezo films: (a) rectified open circuit voltage at wind speeds of 7–8 m/s (b) short-circuit current at wind speeds of 7–8 m/s (c) rectified open circuit voltage at wind speeds of 5–6 m/s (d) short-circuit current at wind speeds of 5–6 m/s (e) rectified open circuit voltage at wind speeds of 3–4 m/s (f) short-circuit current at wind speeds of 3–4 m/s.

5.2. Basic Electrical Output of the Photovoltaic Solar Cell

The bending flexibility suffered when a leaf was affixed with both PV and piezo films. This was mainly due to the inherent stiffness of the solar cell film, and undermined the performance of the piezo films. Consequently, the power output by the piezo films on these leaves was smaller than that of the leaves only affixed with piezo films. When illuminated with an intensity of 478 lumen/m², the solar cell film (110 mm × 50 mm) produced 1.29 mW of power output at a loading resistance of 2 kΩ and a short-circuit current of 1.28 mA with an open circuit voltage of 1.93 V, as shown in Figure 7a.

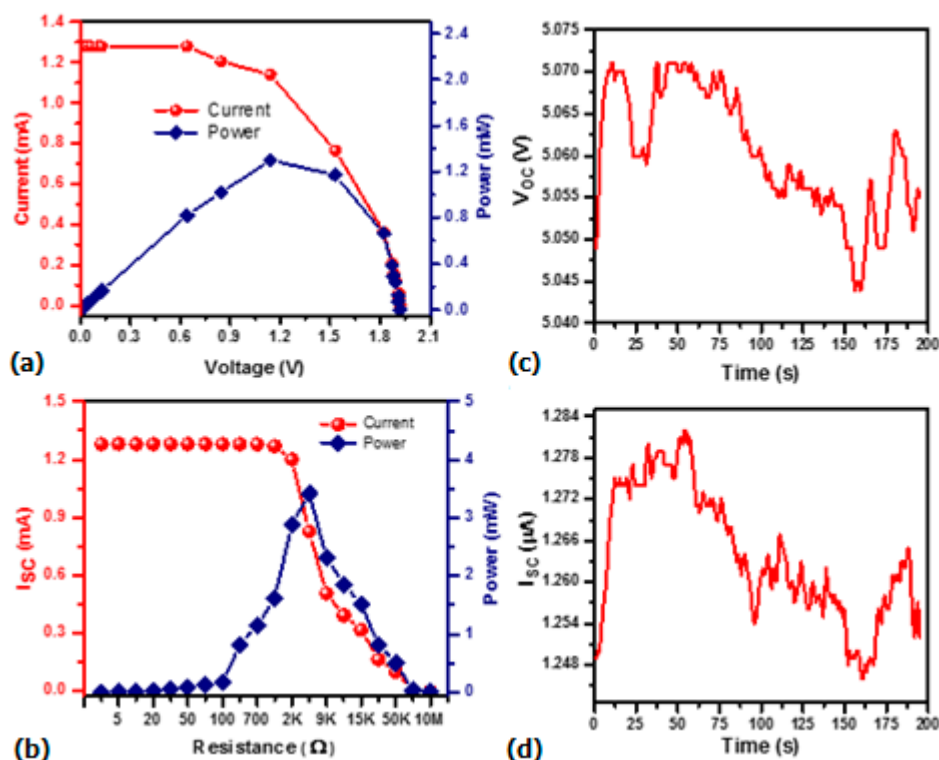


Figure 7. Combined output parameters of the TSHG: (a) combined open circuit voltage (b) I-V characteristics curve of a single PV film (c) combined short-circuit current (d) power output at different loading conditions.

6. Output Measurements of the Tree-Shaped Hybrid Nanogenerator (TSHG)

As the power output of the piezo films were varied with the wind speeds, the power output of the PV films changed in a manner proportionate to the light intensity. Before combining the power output of the piezo and PV films, measurements were made separately on each for comparison. In a luminous environment of 700 lx on an indoor task plane made by fluorescent lamps, the V_{oc} and I_{sc} were 5.06 V and 1.264 mA, respectively. As aforementioned above, the power output of the piezo films was measured at moderate wind speeds of 7–8 m/s. Figure 7 gives an example of the combined power output by the TSHG, where a maximum power output of 3.42 mW at a loading resistance of 5 kΩ was observed as shown in Figure 7b. Figure 7c,d are the results of the combined output for the TSHG consisting of 10 piezo films and three photovoltaic films, which gave the maximum V_{oc} of 5.071 V and maximum I_{sc} of 1.281 mA, respectively. The electric energy saved in the capacitor was discharged through an LED.

Figure 8 shows three different cases of charging the capacitor. Figure 8a shows a fast charging process delivered by the PV films. It took only 15 seconds to charge the capacitor to its saturated electric potential of 5.045 V. Figure 8b shows the case when it was charged only by the generated currents from 10 sheets of piezo films. As shown, the capacitor was charged very slowly. It took 35 min to charge the capacitor up to 4.38 V. As compared to the case of the piezo films, Figure 8c shows

the charging of the capacitor when both outputs are used from the sheets of the piezo and PV films. As shown, no appreciable difference is observed compared to Figure 8a because most of the power is generated by the PV films.

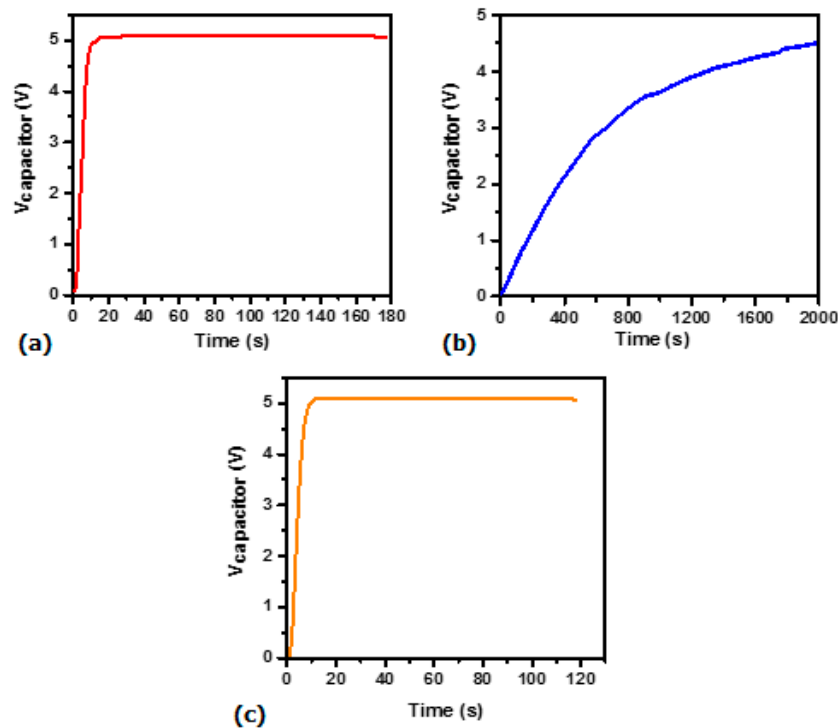


Figure 8. Charging of the capacitor by (a) PV films (b) piezoelectric films (c) combined (TSHG).

7. Conclusions

A small-scale tree-shaped hybrid nanogenerator (TSHG) was designed, fabricated, and tested to analyze its feasibility in harvesting energy from wind and the Sun at the same time. The test results have demonstrated its potential of generating appreciable amount of electricity if sufficient numbers of piezoelectric film sheets are used along with flexible photovoltaic (PV) cells. The power output by these two different distinct types of electric generators were combined to charge a capacitor separately or simultaneously depending on the availability of energy sources. From a series of measurements conducted, it was proven that the TSHG can generate a maximum output power of 3.42 mW with the application of a load resistance of 5 k Ω . The error analysis carried out under different conditions revealed a deviation of ± 0.24 V, which accounts for an error of 4.73%.

Although the power developed by the 10 piezo film sheets was not comparable to that of a PV cell, the present work clearly demonstrated that appreciable power can be produced by the former if more sheets are used. Its total combined output could be sufficient to drive an electronic device and even is comparable to a PV cell. Hybrid operation by implementing two different types of generators enables a rather steady flow of electricity to the capacitor (storage unit) most of the time. During cloudy days with little sunshine and some wind, power will be mostly developed by piezo film sheets. Conversely, on a clear and calm day with little wind, the power will be mostly developed by PV cells. This evidently justifies the hybrid operation of two different types of generators in charging a storage unit as done by the present work, compared to other options of using separate units for different generators.

Author Contributions: Conceptualization, R.A. and W.C.; methodology, R.A. and Y.K.; software, Z.; validation, R.A., Y.K. and Z.; formal analysis, Y.K.; investigation, W.C.; resources, R.A.; data curation, Z.; writing—original draft preparation, R.A.; writing—review and editing, W.C.; visualization, Y.K.; supervision, W.C.; project administration, W.C.; funding acquisition, W.C.

Funding: The authors would like to acknowledge the support from the National Research Foundation of Korea through the Ministry of Science, ICT & Future Planning (Grant Number 2017R1A2A1A05001461).

Conflicts of Interest: The authors declare no conflict of interest.

References

1. Van Atta, L.C.; Northrup, D.L.; Van Atta, C.M.; Van de Graaff, R.J. The Design, Operation, and Performance of the Round Hill Electrostatic Generator. *Phys. Rev.* **1936**, *49*, 761. [[CrossRef](#)]
2. Li, Z.; Chen, J.; Zheng, J.; Pradel, K.C.; Fan, X.; Guo, H.; Wen, Z.; Yeh, M.H.; Yu, C.; Wang, Z.L. High-efficiency ramie fiber degumming and self-powered degumming wastewater treatment using triboelectric nanogenerator. *Nano Energy* **2016**, *22*, 548–557. [[CrossRef](#)]
3. Chen, J.; Zhu, G.; Jing, Q.; Bai, P.; Yang, W.; Qi, X.; Su, Y.; Wang, Z.L. Personalized Keystroke Dynamics for Self-Powered Human-Machine Interfacing. *ACS Nano* **2014**, *9*, 105–116. [[CrossRef](#)] [[PubMed](#)]
4. McEvoy, A.; Castaner, L.; Markvart, T. *Solar Cells: Materials, Manufacture and Operation*, 2nd ed.; Elsevier Ltd.: Oxford, UK, 2012; pp. 3–25. ISBN 9780123869647.
5. Li, G.; Zhu, R.; Yang, Y. Polymer Solar Cells. *Nat. Photonics* **2012**, *6*, 153–161. [[CrossRef](#)]
6. Saga, T. Advances in Crystalline Silicon Solar Cell Technology for Industrial Mass Production. *NPG Asia Mater.* **2010**, *2*, 96–102. [[CrossRef](#)]
7. Scaff, J.H.; Ohl, R.S. The development of silicon crystal rectifiers for microwave radar receivers. *Bell Syst. Tech. J.* **1947**, *26*, 1–30.
8. Razykov, T.M.; Ferekides, C.S.; Morel, D.; Stefanakos, E.; Ullal, H.S.; Upadhyaya, H.M. Solar Photovoltaic Electricity: Current Status and Future Prospects. *Sol. Energy* **2011**, *85*, 1580–1608. [[CrossRef](#)]
9. Badawy, W.A. A review on solar cells from Si-single crystals to porous materials and quantum dots. *J. Adv. Res.* **2015**, *6*, 123–132. [[CrossRef](#)]
10. Schubert, M.B.; Merz, R. Flexible solar cells and modules. *Philos. Mag.* **2009**, *98*, 2623–2644. [[CrossRef](#)]
11. Buresi, M.; Pratesi, F.; Riboli, F.; Wiersma, D.S. Complex photonic structures for light harvesting. *Adv. Opt. Mater.* **2015**, *3*, 722–743. [[CrossRef](#)]
12. Zhang, N.; Chen, J.; Huang, Y.; Guo, W.; Yang, J.; Du, J.; Fan, X.; Tao, C. A Wearable All-Solid Photovoltaic Textile. *Adv. Opt. Mater.* **2016**, *28*, 263–269. [[CrossRef](#)] [[PubMed](#)]
13. Ye, M.; Hong, X.; Zhang, F.; Liu, X. Recent advancements in perovskite solar cells: Flexibility, stability and large scale. *J. Mater. Chem. A* **2016**, *4*, 6755–6771. [[CrossRef](#)]
14. Peng, M.; Liu, Y.D.; Yu, A.F.; Zhang, Y.; Liu, C.H.; Liu, J.Y.; Wu, W.; Zhang, K.; Shi, X.; Kou, J.; et al. Flexible self-powered GaN ultraviolet photoswitch with piezo-phototronic effect enhanced on/off ratio. *ACS Nano* **2015**, *10*, 1572–1579. [[CrossRef](#)] [[PubMed](#)]
15. Wang, Z.L. Triboelectric nanogenerators as New Energy Technology for Self Powered Systems and as active Mechanical and Chemical Sensors. *ACS Nano* **2013**, *7*, 9533–9557. [[CrossRef](#)]
16. Pan, C.; Niu, S.; Ding, Y.; Dong, L.; Yu, R.; Liu, Y.; Zhu, G.; Wang, Z.L. Enhanced Cu₂S/CdS Coaxial Nanowire Solar Cells by Piezo-Phototronic effect. *Nano Lett.* **2012**, *6*, 3302–3307. [[CrossRef](#)] [[PubMed](#)]
17. Jiang, C.; Jing, L.; Huang, X.; Liu, M.; Du, C.; Liu, T.; Hu, W.; Wang, Z.L. Enhanced Solar Cell Conversion Efficiency of InGa_N/Ga_N Multiple Quantum Wells by Piezo-Phototronic Effect. *ACS Nano* **2017**, *11*, 9405–9412. [[CrossRef](#)] [[PubMed](#)]
18. Zhu, L.; Wang, L.; Pan, C.; Chen, L.; Xue, F.; Chen, B.; Yang, L.; Su, L.; Wang, Z.L. Enhancing the Efficiency of Silicon-Based Solar Cells by the Piezo-Phototronic Effects. *ACS Nano* **2017**, *11*, 1894–1900. [[CrossRef](#)] [[PubMed](#)]
19. Xue, F.; Yang, L.; Chen, M.; Chen, J.; Yang, X.; Wang, L.; Chen, L.; Pan, C.; Wang, Z.L. Enhanced photoresponsivity of the MoS₂-Ga_N heterojunction diode via the piezo-phototronic effect. *NPG Asia Mater.* **2017**, *9*, e418. [[CrossRef](#)]
20. Chen, J.; Huang, Y.; Zou, H.; Tao, C.; Fan, X.; Wang, Z.L. Micro-cable structured textile for simultaneously harvesting solar and mechanical energy. *Nat. Energy* **2016**, *138*, 16138. [[CrossRef](#)]
21. Rørvik, P.M.; Grande, T.; Einarsrud, M.A. One dimensional nanostructures of ferroelectric perovskites. *Adv. Mater.* **2011**, *23*, 4007–4034. [[CrossRef](#)]
22. Wang, Z.L. From nanogenerators to piezotronics—A decade long study of ZnO nanostructures. *MRS Bull.* **2012**, *37*, 814–827. [[CrossRef](#)]

23. Wang, Z.L.; Song, J. Piezoelectric Nanogenerators Based on Zinc Oxide Nanowire Arrays. *Science* **2006**, *312*, 242–246. [[CrossRef](#)] [[PubMed](#)]
24. Gu, L.; Cui, N.; Cheng, L.; Xu, Q.; Bai, S.; Yuan, M.; Wu, W.; Liu, J.; Zhao, Y.; Ma, F.; Qin, Y.; et al. Flexible fiber nanogenerator with 209 V output voltage directly powers a light-emitting diode. *Nano Lett.* **2013**, *13*, 91–94. [[CrossRef](#)] [[PubMed](#)]
25. Kwon, J.; Seung, W.; Sharma, B.K.; Kim, S.W.; Ahn, J.H. A high performance PZT ribbon-based nanogenerator using graphene transparent electrodes. *Energy Environ. Sci.* **2012**, *5*, 8970–8975. [[CrossRef](#)]
26. Jung, J.H.; Lee, M.; Hong, J.I.; Ding, Y.; Chen, C.-Y.; Chou, L.J.; Wang, Z.L. Lead-free NaNbO₃ nanowires for a high output piezoelectric nanogenerator. *ACS Nano* **2011**, *5*, 10041–10046. [[CrossRef](#)] [[PubMed](#)]
27. Zeng, W.; Tao, X.M.; Chen, S.; Shang, S.; Chan, H.L.; Choy, S.H. Highly durable all-fiber nanogenerator for mechanical energy harvesting. *Energy Environ. Sci.* **2013**, *6*, 2631–2638. [[CrossRef](#)]
28. Kellogg, W.; Nehrir, M.H.; Venkataramanan, G.; Gerez, V. Optimal unit sizing for a hybrid wind/photovoltaic generating system. *Electr. Power Syst. Res.* **1996**, *39*, 35–38. [[CrossRef](#)]
29. Oh, S.J.; Han, H.J.; Han, S.B.; Lee, J.Y.; Chun, W.G. Development of a tree-shaped wind power system using piezoelectric materials. *Int. J. Energy Res.* **2010**, *34*, 431–437. [[CrossRef](#)]
30. Han, M.; Zhang, X.S.; Meng, B.; Liu, W.; Tang, W.; Sun, X.; Wang, W.; Zhang, H. r-Shaped Hybrid Nanogenerator With Enhanced Piezoelectricity. *ACS Nano* **2013**, *7*, 8554–8560. [[CrossRef](#)]
31. Hassan, G.; Khan, F.; Hassan, A.; Ali, S.; Bae, J.; Lee, C.H. A flat-panel-shaped hybrid piezo/triboelectric nanogenerator for ambient energy harvesting. *Nanotechnology* **2017**, *28*, 175402. [[CrossRef](#)]
32. Boston Piezo-Optics Inc. An Introduction to Transducer Crystals. Available online: <http://www.bostonpiezooptics.com/?D=6> (accessed on 2 January 2019).



© 2019 by the authors. Licensee MDPI, Basel, Switzerland. This article is an open access article distributed under the terms and conditions of the Creative Commons Attribution (CC BY) license (<http://creativecommons.org/licenses/by/4.0/>).